

# Four-Dimensional 8-bit Modulation with KP4 Non-binary FEC for Short-Reach Coherent Optical Transmissions

Liangjun Zhang<sup>1</sup>, Hung-Chang Chien<sup>2</sup>, Yi Cai<sup>2</sup>, Weiming Wang<sup>1</sup>, Weiqin Zhou<sup>1</sup>, and Zihe Hu<sup>1</sup>

<sup>1</sup> ZTE Corporation, Huashiyuan Rd, Donghu H.D.Z., Wuhan, 43004, China

<sup>2</sup> ZTE (TX) Inc., 65 Madison Ave., Morristown, NJ07960, USA  
zhang.liangjun1@zte.com.cn

**Abstract:** C4-256 four-dimensional 8-bit modulation with non-binary FEC is firstly proposed and demonstrated for coherent optical transmissions, which outperforms its PM-16QAM counterpart by 0.7-dB for required OSNR at  $10^{-8}$  post-FEC BER.

**OCIS codes:** (060.0060) Fiber optics and optical communications; (060.4080) Modulation

## 1. Introduction

Employing higher order modulation formats such as polarization multiplexed (PM)- $m$ QAM ( $m = 16, 64$  etc) can improve the spectral efficiency (SE) and system transmission capacity. However, spectral efficiency and power efficiency might be essentially a pair of contradictions, i.e, higher order modulation formats typically give lower asymptotic power efficiency (APE) which limits transmission distance. Multi-dimensional modulation formats simultaneously apply multiple degrees of freedom including orthogonal states of optical field, polarization states and time slots to modulate data [1]. This allows the minimum Euclidean distance to be maximized at a given SE, and thus increase the APE. Although a multi-dimensional modulation format as a result of higher APE can have better symbol error rate (SER) performance compared to a corresponding PM- $m$ QAM, it may experience higher loss during symbol-to-bit de-mapping if Gray mapping is not applicable to its case. This would explain why binary forward error correction (FEC) cannot fully exploit the performance advantages of multi-dimensional modulation as being demonstrated in prior research studies [2].

In this paper, we propose to use non-binary FEC along with four-dimensional (4D) modulation for coherent optical transmissions. An optimized 4D 8-bit modulation format namely C4-256 is selected for this research study, which, according to sphere packing theory, has exactly the same SE of 4 bits/symbol/polarization with that of PM-16QAM and exhibits 1.71 dB APE gain over PM-16QAM [3]. We compare through simulation the performance of C4-256 and PM-16QAM with binary and non-binary FEC, respectively. The non-binary FEC of in the study includes the standardized and widely adopted RS(544, 514) KP4 FEC for point-to-point Ethernet interfaces. Experimental results also confirm that C4-256 outperforms PM-16QAM at the pre-FEC SER threshold of the KP4 FEC, making it promising for short-reach coherent optical transmissions.

## 2. Mutual Information of 8-bit Modulation: C4-256 vs. PM-16QAM

C4-256 has 256 constellation points in a 4D space. Such a 4D space may correspond to the four signal modulation tributaries: XI, XQ, YI, and YQ, in a typical coherent transceiver architecture. A 3D projection view of C4-256 is shown in Fig. 1(a), where low-energy symbols are utilized more often than others. The size of each constellation point indicates its probability of occurrence. Furthermore, the 2D projection view of C4-256 (in one polarization) looks like a 32QAM constellation with probabilistic shaping, and its probability density distribution is depicted in Fig. 1(b). Note that C4-256 simply utilizes the correlation of two polarization states to achieve such probability density distribution. Neither a distribution matcher (DM) with additional overhead nor a special probability amplitude shaping (PAS) scheme for combining with FEC codes are required as compared to typical probabilistic shaping approaches. The specific coordinates of the constellation points are described in detail in [3].

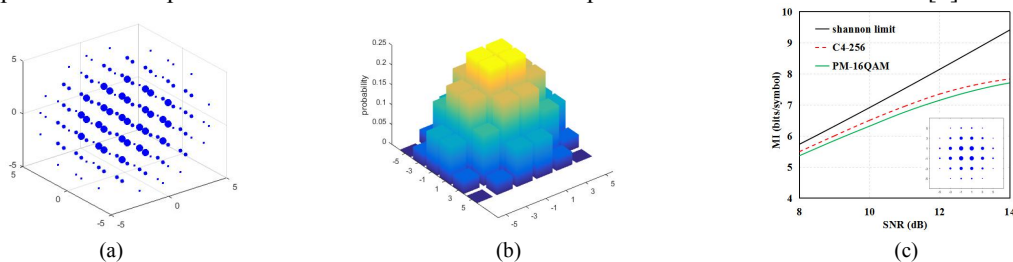


Fig. 1 (a) The 3D projection view, (b) the 2D probability distribution, and (c) the MI of C4-256 and PM-16QAM

The capacity of arbitrary modulation format  $\chi$  can be numerically calculated by maximizing mutual information (MI), as follows

$$I(X;Y) = \sum_{x \in \chi} P_X(x) \int P_{Y|X}(y|x) \log_2 \frac{P_{Y|X}(y|x)}{P_Y(y)} dy \quad (1)$$

where  $X$  and  $Y$  are the constellation symbols and channel output [4]. We use Monte Carlo numerical methods to calculate the MI of C4-256 and PM-16QAM in Gaussian channel. From Fig. 1(c), we can see C4-256 has better theoretical MI in high SNR region. This is explained by the increase in minimum Euclidean distance of C4-256 with respect to PM-16QAM. Since the MI measures the similarity of transmitted and detected symbols rather than bits, the theoretical bound is thus more meaningful on forward error correction scheme that operates on a symbol level, i.e., non-binary FEC [5].

### 3. Simulation Setup and Experimental Test Bed

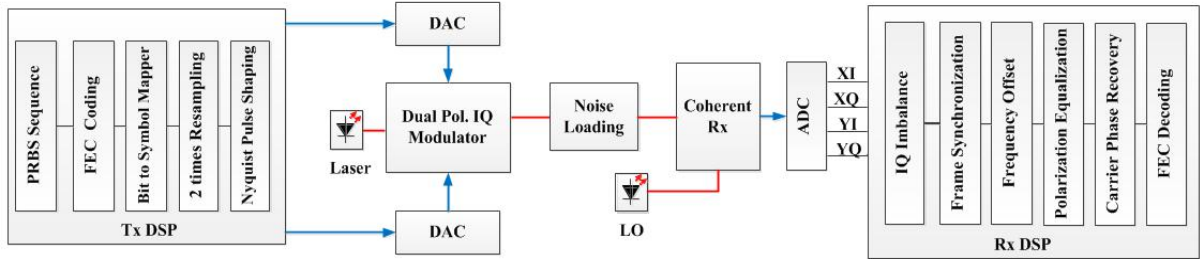


Fig. 3. Simulation setup for C4-256 and PM-16QAM transmission

Simulations are first performed to compare the performance of C4-256 and PM-16QAM. Fig. 3 shows the back-to-back simulation setup for the C4-256 and PM-16QAM systems. A pseudo-random bit sequence (PRBS31) is generated and FEC coded for both formats. The sampling rates of ADC and DAC are 112 GS/s, and the coded bits are mapped to generate symbols followed by 2 times upsampling and Nyquist shaping with a 0.2 roll off factor, generating symbols at 56 GBd. The PM-16QAM case uses Gray mapping while the C4-256 one employs numerically optimized bit mapping. In addition, 6 training symbols are inserted every 122 data symbols. The net data rate when coded with RS(544, 514) KP4 FEC is  $56 \times 8 \times (122/128) \times (514/544) \approx 403$  Gb/s. The 4-way components of signal are fed into a dual polarization IQ modulator generating C4-256 or PM-16QAM optical signal with a fixed output power of 0 dBm at 1549.32 nm. The linewidth of Tx laser and local oscillator (LO) is 100 kHz and the frequency offset is set at 1 GHz. The noise loading block comprises an attenuator and an erbium doped fiber amplifier (EDFA).

In receiver-end digital signal processing, most modules are the same for both modulation formats. The IQ imbalance is compensated using Gram-Schmidt orthogonalization procedure (GSOP) algorithm. Then we use the training sequence to compensate the frequency offset and get the initial polarization equalization coefficient. The carrier phase noise is estimated and compensated by blind phase search algorithm. After carrier phase recovery, an adaptive equalizer based on decision directed least-mean square is used for further equalization. For both formats, the maximum likelihood algorithm is performed to decode symbol before FEC decoding. The experimental test bed has all the components in the simulation setup with the same settings. However, due to the bandwidth limitation of ADC, the experiment symbol rate is operated at 28 GBd. The DAC and ADC in the experiment are operated at 92 GS/s and 160 GS/s with 20 GHz and 40 GHz analog bandwidths, respectively.

### 4. Results and Discussion

The simulated pre-FEC SER and BER performance of C4-256 and PM-16QAM are shown in Fig. 4(a) and Fig. 4(b). We see that C4-256 has more than 1 dB gain in OSNR compared to PM-16QAM and the gain becomes larger at lower SER. However, due to the loss of C4-256 in its symbol-to-bit conversion, its BER is higher than PM-16QAM at high SERs. Hence, we choose a non-binary and a binary FEC codes with similar code length and overhead to compare post-BER performance, namely RS (255, 231) and BCH (2047, 1849). From Fig. 4(c) we can see C4-256 combined with RS (255, 231) has the best sensitivity among the four combinations. It has about 0.3 dB gain compared with PM-16QAM using BCH(2047,1849) for  $10^{-7}$  post-FEC BER. In addition, Fig. 4(d) shows the C4-256 has about 0.7dB gain compared to PM-16QAM at  $10^{-8}$  post-FEC BER when using KP4 RS(544,514) codes.

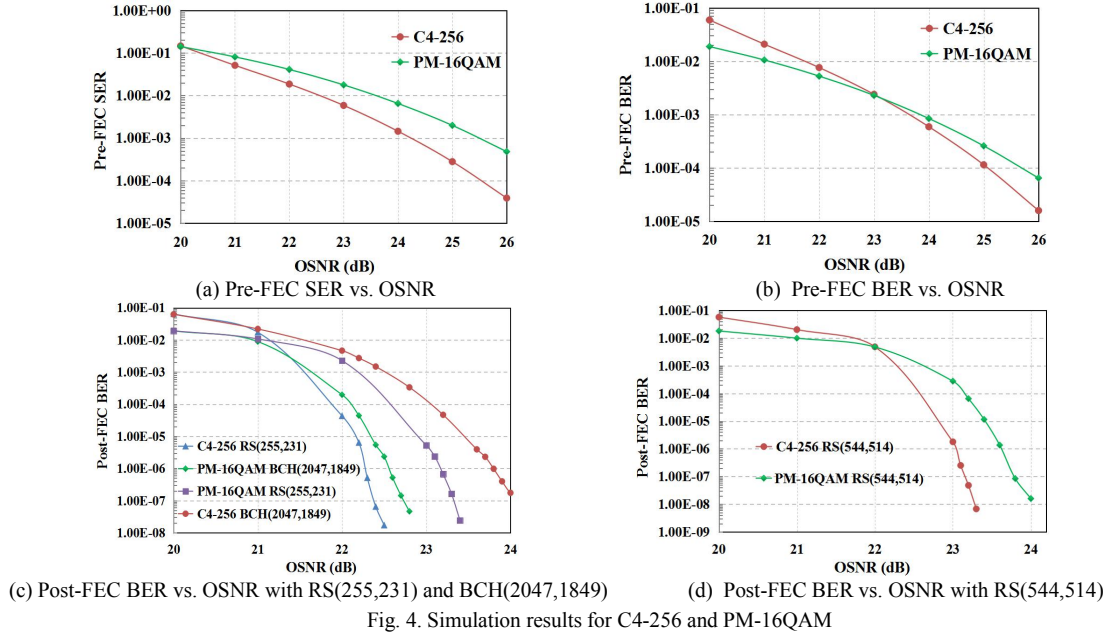


Fig. 4. Simulation results for C4-256 and PM-16QAM

Fig. 5 shows the measured pre-FEC SER as a function of OSNR for both cases. Drawn from the simulation results of Fig. 4(a) and 4(d), a pre-FEC SER threshold for predicting KP4 post-FEC BER of below  $10^{-8}$  is around  $5 \times 10^{-3}$ . Given that, the experimental results show that C4-256 exhibits  $\sim 0.7$  dB gain in required OSNR compared to PM-16QAM. Inset (a) and (b) illustrate the measured 1D driving signal of 28 GBd C4-256 and PM-16QAM at the DAC output, respectively. In addition, inset (c) and (d) display the measured x-polarization constellations of C4-256 and PM-16QAM, respectively, at 24 dB OSNR. The received optical power (ROP) measured at pre-FEC SER threshold for the C4-256 case is around  $-31.3$  dBm. As the output power of commercially available coherent transmitters could range from  $-10$  to  $0$  dBm, the proposed scheme could potentially support a single-wavelength 200GbE point-to-point link having a loss budget of  $21.3$  dB  $\sim 31.3$  dB.

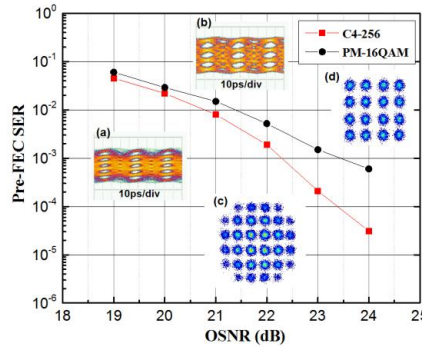


Fig. 5. Measured Pre-FEC SER vs. OSNR for C4-256 and PM-16QAM

## 5. Conclusion

We have calculated the MI of C4-256 to show that C4-256 is closer to the channel capacity than PM-16QAM. Simulation are performed to compare the transmission performance of C4-256 and PM-16QAM. Thanks to higher power efficiency, C4-256 has better SER performance than PM-16QAM. Therefore, non-binary FEC is more suitable for C4-256. The simulation results show that the C4-256 has about  $0.7$  dB gain compared to PM-16QAM at  $10^{-8}$  post-FEC BER when employing non-binary RS(544,514) codes.

## 6. References

- [1] D. S. Millar, et al., "High-dimensional modulation for coherent optical communications systems," *Opt. Exp.*, vol. 22, pp. 8798-8812, 2014.
- [2] T. A. Eriksson, et al., "Experimental Investigation of a Four-Dimensional 256-ary Lattice-based Modulation Format," *Proc. OFC 2015*, W4K.3.
- [3] E. Agrell, "Database of sphere packings," <http://codes.se/packings/>
- [4] T. Fehenberger, et al., "On achievable rates for long-haul fiber-optic communications," *Opt. Exp.*, vol. 23, pp. 9183-9191, 2015.
- [5] D. zou, et al., "FPGA-based LDPC-coded APSK for optical communication systems," *Opt. Exp.*, vol. 25, Issue 4, pp. 3133-3142, 2017.